2024 IEEE International Conference on Robotics and Automation (ICRA 2024)
May 13-17, 2024. Yokohama, Japan

Design of Morphable StateNet Based on Pseudo-Generalization of Standing Up Motions for Humanoid with Variable Body Structure

Tasuku Makabe[1], Kei Okada[1] and Masayuki Inaba[1]

Abstract— **In this paper, we explain the Morphable StateNet as the StateNet with pseudo-generalized behaviors for robots with various degree-of-freedom arrangements and link lengths. Pseudo-generalization is performed by analytically calculating joint angles that satisfy the desired support conditions, focusing on link lengths and antigravity joints that contribute to motion, with constraints placed on the contact conditions between the environment and the robot body. We apply Morphable StateNet to the standing-up motion of humanoids with variable body structures and conduct evaluation experiments. We have demonstrated the usefulness of the proposed method in environments with low friction coefficients with the environment by conducting evaluations using both a simulator and an actual humanoid.**

I. INTRODUCTION

In recent years, research has been conducted on the use of multi-degree-of-freedom humanoids to replace hazardous tasks and assist with household tasks in real environments. Humanoids can move in confined environments due to the DOF of their leg structures and small footprints, but unlike mobile manipulators, they are not statically stable without control. However, it is difficult to generalize the motion generation because the motion involves multiple points of contact and various transitions of the contact state with the environment. In conventional methods, sequences of joint angles suitable for the body structure of a robot with a specific link length are prepared in advance, and the posture transitions are handled as networks (StateNet) to execute the motion to be executed from the current and target states[1], [2]. However, there are problems that it is difficult to handle diverse body geometries during generating whole-body movements. Since the joint angle sequences for posture transitions are often fixed in conventional StateNet, the configuration of a method as general as possible for limbs with varying geometry and link lengths is necessary to apply it to a variety of robots, and we need to design reasonable heuristics to easily determine motion trajectories.

In this study, we propose Morphable StateNet as a StateNet equipped with such edges that can be generalized by constraining the contact state and the joints to be driven to simplify the generation of trajectories for whole-body posture transition movements such as standing up. For verifying the usefulness of Morphable StateNet, we realize that standing-up motions include morphable motions using humanoids with variable body structures such as limb lengths and DOFs.

[1] Authors are with Department of Mechano-Informatics, Graduate School of Information Science and Technology, The University of Tokyo, 7-3-1 Hongo, Bunkyo-ku, Tokyo, 113-8656, Japan. [makabe, k-okada, inaba]@jsk.t.u-tokyo.ac.jp

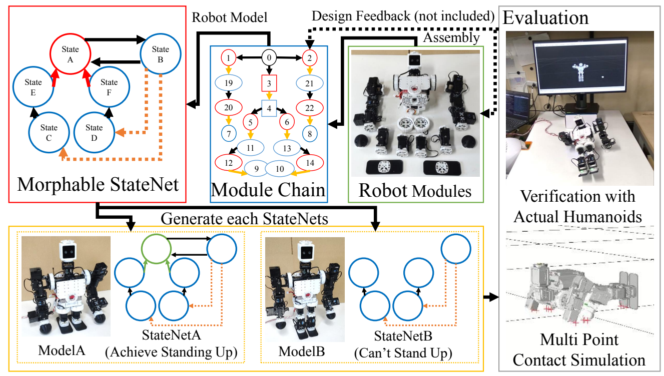

Fig. 1: Concept of Whole System of Morphable Statenet for Robots with Variable Body Structure.

II. RELATED WORKS AND OUR CONTRIBUTION

A. Related Works

Humanoids have been using the StateNet to handle recovery from failed states such as falls, transitions to specific movement postures, and task execution in general[1]. In recent years, they have been adapted to sturdy life-size humanoids[2], but regardless of scale, changes in body geometry and degree-of-freedom arrangements are likely to make it difficult to use existing networks. This research aims to pseudo-generalize the edge of StateNet, which corresponds to posture transitions between states at small scales, and to use the body shape representations for StateNet and adapt StateNet to diverse body shapes.

Many humanoids have been proposed that are equipped with flexible materials on their body surfaces that allow them to explore standing-up trajectories while keeping their entire body in contact with the environment[3], [4]. Since adapting position control for robots with flexible exteriors is difficult, it is necessary to consider contact state transitions in joint torque space. Hardware capable of torque measurement and control has been proposed, such as motor-level torque control with a joint structure with high backdrivavirity[5], or joints with additional torque measurement capability[6]. This study attempts pseudo-generalizations of the standing-up motion within the joint angle space by using joint angle sensors, which many robots are equipped with at a minimum with constraints on the contact points.

In planning multi-point contact motion by a robot with multiple degrees of freedom, such as standing up, some methods search for contact points from the mesh surface of contact links[7] or search for a whole-body posture with a safe contact state by evolutionary computation as a method to easily provide a contact state[8], [9], [10]. Since most of the conventional methods are costly methods using optimization and evolutionary computation, this method examines and verifies a simplified method that is valid for humanoids that can respond to changes in body structure during movement.

Many humanoids can take different forms of movement for different purposes by changing their state of contact with the environment. Humanoids that aim to expand mobility with wheels include the CHIMP[11] and HUBO[12]. The ability to realize movements in disaster relief environments has been extended by expanding the support area and improving stability during movement by transforming into a shape with wheels. Since the body structure of these robots does not change, conventional StateNet methods can be applied to them. In this study, we aim to realize pseudo-generalized standing-up motions with a single robot that has joint mechanisms[13] on its body as well as modular robots, and whose body structure changes.

B. Our Contribution

The contributions of this paper are as follows

1) Proposed Morphable StateNet, with pseudo-generalized actions using body structure information.
2) Verified the proposed method for getting up motion using a robot that can realize various body structures.

Regarding pseudo-generalization of StateNet, this study focuses on the fact that bodied similar to human shapes can be typified as a contact state transition between the environment and the body, and proposes Morphable StateNet as a generalization of trajectories in such typical contact point transitions. For verification using an actual robot with various body structures, we will generate configurable robot models and verify them in a simulator using a system that switches models of the actual robot while the human interactively configures them[13]. We show how the entire system can be configured to verify the proposed method using robots with a variety of body shapes.

III. Design of Morphable StateNet

We describe the design of Morphable StateNet in this chapter. First, we explain pseudo-generalizations after modeling the getting-up deformation behavior of a humanoid. Next, the Module Chain, a graph structure for representing a body with connected modules, is explained and its correspondence with the modeling of the getting-up deformation behavior is shown. Finally, we explain Morphable StateNet as the StateNet that includes pseudo-generalization behavior as edges.

A. Modeling and Pseudo-Generalization of Getup Motion

In this study, the entire operation is decomposed into the following two elements

1) Motion to add or remove new support points.
2) Motion to manipulate the center of gravity position by driving joints that contribute to weight bearing without changing the support state

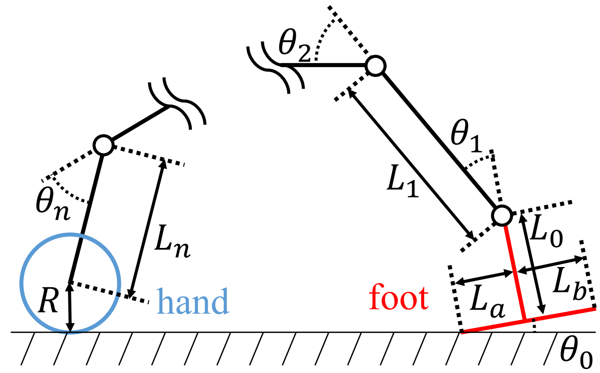

Fig. 2: Coordinate System of Preudo-Generalization.

In many cases, especially in planning the transition of the contact state between the environment and the robot body, the cost of the search is high because it is necessary to keep considering discrete state transitions until the goal is achieved. Adapting this method to general robots is a difficult problem because it is necessary to consider link geometries that make it difficult to transition the support region while maintaining the contact state between the environment and the robot. Therefore, this study aims at motion generation focusing only on the manipulation of geometric conditions, assuming that only the slippery end links are in contact with the environment.

The pseudo-generalization of the standing-up deformation motion focusing on geometric body manipulation in humanoids is shown in the coordinate system Fig.2. In this study, we focus on the property that the joints contributing to the standing-up motion of humanoids are concentrated in the antigravity joints, and consider them on a two-dimensional plane to show them analytically. First, assume a spherical end-effector with a constant radius R and a foot flat with lengths L_a, L_b and height to the nearest neighbor L_0. Assume that there are n antigravity joints, with each joint angle as θ_1 θ_n and the angle between the sole and the ground as θ_0. Also, let L_i be the length between the antigravity joints i and $i+1$. For example, in one of the configuration examples of humanoids handled in this study shown in figreffigure:pseudo-generalization, $n=4$ because there are 1 antigravity joints in the legs and 3 in the arms. The geometric constraints during the standing-up motion shown in Fig.2 are indicated by the equation (1). In this study, we consider the case where $0 <= \theta_0 < \frac{\pi}{2}$ and the ground is contacted at the tip of the foot flat. In this example, we consider the case where the toes contact the ground, but if the heel side contacts the environment, L_a should be replaced with L_b, and the coordinate system for the angle should be changed.

$$L_a \sin\theta_0 + \sum_{i=0}^{n} L_i \cos(\sum_{j=0}^{i} \theta_j) = R_n \ (0 <= \theta_0 < \frac{\pi}{2}) \quad (1)$$

For example, if $\theta_0 = 0$ to make the foot plane parallel to the ground, $\theta_0 = 0$ is an n-variable identity, and $n-1$ joint angles are determined, the remaining joint angles may be calculated analytically, depending on link length.

In addition, in the support region transition described below, the distance L_s from the center of the foot flat to the tip of the hand, which is related to the length of the support region in the left-right direction of the paper, is expressed by the following equation.

$$\sum_{i=1}^{n} L_i \sin(\sum_{j=1}^{i} \theta_j) = L_s \ (\theta_0 = 0) \quad (2)$$

B. Robot Body Modeling with Module Chain

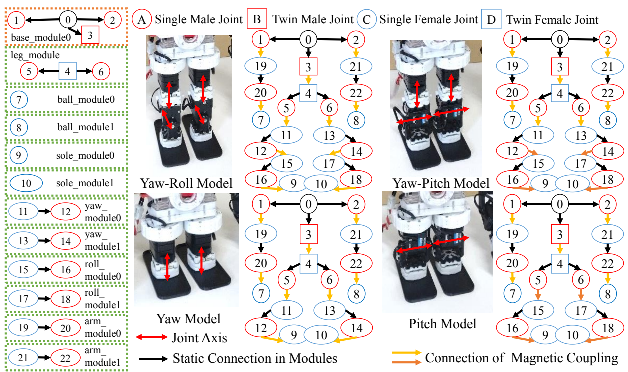

Fig. 3: Module Chains of Transformable Humanoid.

TABLE I: Configuration of Antigravity Joints and Links.

Config Name	Antigravity Joints, Length ([mm])
Yaw-Roll	Foot ($L_0 = 240.5$), Shoulder ($i = 1, L_1 = 58.0$), Elbow ($i = 2, L_2 = 61.0$), Wrist ($i = 3, L_3 = 58.5$)
Yaw-Pitch	Foot ($L_0 = 43.5$), Ankle ($L_1 = 197.0$) Shoulder ($i = 2, L_2 = 58.0$), Elbow ($i = 3, L_3 = 61.0$), Wrist ($i = 4, L_4 = 58.5$)
Yaw	Foot ($L_0 = 164.5$), Shoulder ($i = 1, L_1 = 58.0$), Elbow ($i = 2, L_2 = 61.0$), Wrist ($i = 3, L_3 = 58.5$)
Pitch	Foot ($L_0 = 43.5$), Ankle ($L_1 = 140.5$) Shoulder ($i = 2, L_2 = 58.0$), Elbow ($i = 3, L_3 = 61.0$), Wrist ($i = 4, L_4 = 58.5$)
Fixed Links	Hand ($R = 20.0$), Foot ($L_a = L_b = 50.0$)

We use Module Chains to model the robot body. The robot model of the real robot can be reconstructed from the Module Chain as shown in Fig.3. From the robot model, the number of antigravity joints n, which are variables in the Subsection III-A, the links between joints L_i, geometric parameters R_n, L_a, L_b, θ_1 to θ_n, and an equation with indirectly controllable variables θ_0 can be determined. The antigravity joints and link lengths for the robots with four different leg structures handled in this study are shown in Table.I.

C. Morphable StateNet for Getup Motion and Evaluation of Feasibility of Edge

Morphable StateNet in the standing up operation to Fig.4 consists of the following.

1) Robot falls down
2) Determine the state of falling based on the posture
3) Transition to a posture in which both hands and both flats are in contact with the environment according to the direction of the fall

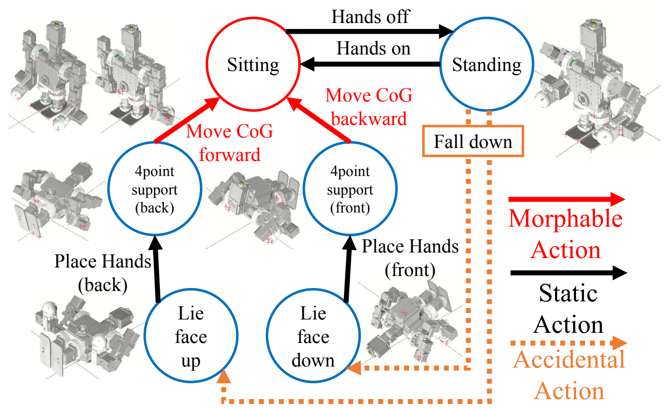

Fig. 4: Overview of Morphable StateNet.

4) Transition to a posture in which both feet are parallel to the floor
5) Transition to the point where the support area is minimized without tipping over
6) Moves to an upright posture with the fingertips off the floor

For 1, 2, and 3, according to the StateNet principle, the robot transitions from the tipping-over state to the nearest neighbor state and then performs a fixation movement to transition to a state with both hands and feet in contact with the environment (Place Hands (front, back)). These are static actions in that robots move only the arm degrees of freedom, which do not change in the robot model handled in this study. For 4, 5, and 6, these are the Morphable Actions proposed in this study, which are pseudo-generalized Morphable Actions (Move CoG forward, backward) for the constructed robot model and the terminal posture (Sitting) of the Morphable Action. The robot attempts to contact the ground with its entire foot flat parallel to the ground while keeping both arms and legs attached to the environment (Motion a) and transitions to a smaller support area to the extent that it does not fall over (Motion b), and transitions to an upright motion by releasing its arms (Motion c). These Motion a, b, and c are trajectory planning using the analytical constraints on the contact between the environment and the robot body as shown in(1), where each action is assumed to be performed when the previous action is feasible and accomplished, and the next action is assumed to be performed when the previous action is feasible and accomplished, each of which is defined by(1), and the variables to be fixed and the variables to be moved are arbitrarily set so that each movement satisfies (1).

The value for the joint angle θ_j that satisfies these actions may not exist depending on the link length L_i, R and the range of motion of the joint. In such cases, the action is considered unfeasible and the Morphable Action in the corresponding robot is considered unfeasible. In this study, the validity of the edge is confirmed by determining whether a Morphable Action that is executable in one configuration of the robot is executable in another configuration.

IV. Hardware System of Transformable Humanoid and Generation Method of Module Chain

This chapter describes the hardware system of the humanoid robot with magnetic couplings. First, we present an overview of the hardware system for the variable morphology humanoid used. Next, we explain the magnetic couplings for variable body structure and the method of module recognition and generation of module chains using the sensors included in the mechanism.

A. Overview of Robot System

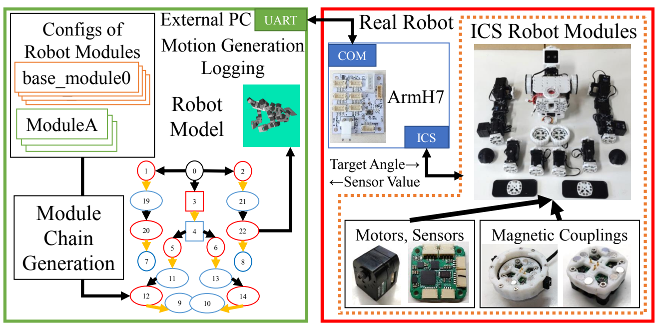

Fig. 5: System of Robots with Variable Structure.

The robot system proposed in this paper is equipped with TTL serial servo motors[14] and multi-sensor boards[15] as devices, and each module has magnetic couplings. The control board (kondoh7) and the motor/sensor device are connected in a daisy chain with three lines: VCC, the signal line (UART half duplex), and GND. Since VCC, signal line, and GND all conduct in the same daisy chain, communication between the control board and the device is independent of the wiring topology, and conversely, it is possible to detect when communication is lost, which is used to detect variable body structures in this study.

B. Design of Attach-Lock-Detachable Magnetic Coupling

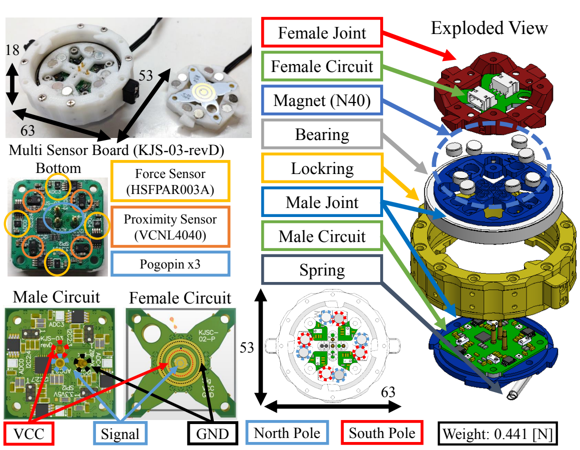

Fig. 6: Hardware Design of Magnetic Coupling.

We show the design of magnet couplings in Fig.6. This mechanism consists of an electrical connection mechanism with a pair of interface boards (female and male boards) and a mechanical joint mechanism with a permanent magnet and a claw mechanism for fixation. For the electrical connection mechanism, the female board has only a concentric pad (front) and a connector (back), while the male board is the sensor board proposed in [15] with an additional pogo pin on the sensor surface. The sensor board is equipped with an infrared proximity sensor[16], which can detect the type and direction of the object being joined by detecting the position and number of holes in the female board. Also, regarding the pogo pins on the male board and the concentric pads on the female board, the three-pole communication system (VCC, signal line, and GND) corresponds to each of them, and it is possible to maintain continuity regardless of the angle at which they are connected. Regarding the mechanical connection mechanism, all mechanisms have a female-free shape with up to eight neodymium magnets (N40, $Radius, Height = 2.5[\text{mm}]$) in alternate directions, enabling alignment and connection to be maintained by magnetic force while receiving shear direction force with the exterior shape. We show the details and functions of this mechanism in another paper[13].

C. Method of Module Chain Generation

We show below the steps to configure Module Chains.

1) Obtain the IDs of devices that exist in the communication system.
2) Verify the ID of each module with the assumed modules.
3) Output the connection status between modules as TF and join the whole

First, the IDs of devices existing in the communication system are acquired. The system used in this research does not explicitly provide information on devices that can be connected to the communication system but identifies existing devices by attempting to communicate with each device from the main control board when the board is energized or at a user's discretion.

Next, from the list of identified device IDs, the connected modules are estimated. In this study, we assume the modules shown in Fig.6 as a set to validate the proposed method, and each of them is assigned a device ID to avoid collision.

Finally, the connection state between modules is output as TF[17]. Here, the relative positional posture between the connection points is output as TF, but to do so, it is necessary to determine the order in which the modules themselves are connected and to describe the Module Chain. Since multiple modules may be connected in the same communication system in the module set prepared in this research, the order of individual modules is identified by changing the arrangement of holes in each module and detecting the difference with the proximity sensor equipped with magnetic couplings.

V. Experiment

We explain the results of experiments to verify the proposed method. First, we show the whole-body visualization experiment using an actual robot to generate Module Chains when modularized body structures are recombined in various ways. Next, we conduct evaluating experiments using the simulator for Morphable StateNet composed of pseudo-generalized edges for each certain body structure. Finally, we show an experiment to realize a standing-up deformation motion by transforming the edges according to the generated Module Chain using an actual robot.

A. Evaluation of Method of Module Chain Generation

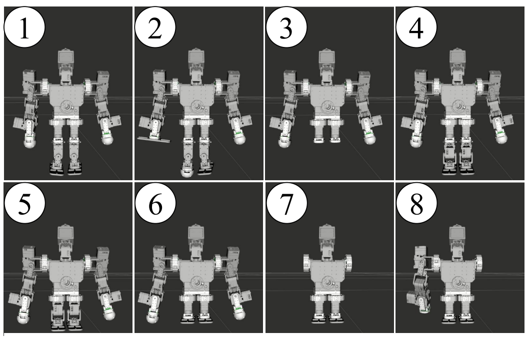

Fig. 7: Visualization of Module Chain of Real Robot.

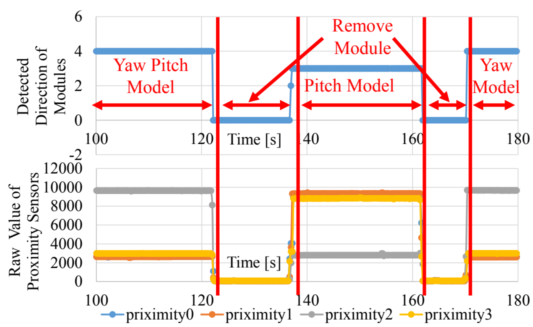

Fig. 8: Proximity Sensor Values of Magnetic Coupling at Rleg Crotch.

We evaluated the generation of Module Chain in experiments with visualizing interactively recombined body structures. The appearance of the experiment is shown in Fig.7 and the results of the experiment are shown in Fig.8. As the experimental results show, it is possible to visualize the transformation of the robot model in response to the recombination of the actual device. First, for the spherical hand and foot parts that do not contain electrical devices, we can see that by associating the holes in the parts with each element, the proximity sensor can recognize and distinguish the placement of the holes even if each element is replaced (ⓢcriptsize2). Next, regarding the leg DOF placement, we can continuously realize and visualize four different DOF configurations by recombining the leg DOFs (yaw, pitch, yaw-pitch, yaw-roll ③$-$ *raise*0.2*ex*⑥). In this experiment, although the separation was detected stably when the module was removed, there were cases where communication between the control board and the device was not established when a new module was installed. We can observe that devices originally connected to the same communication system were also affected, but it was found that connection could be established by increasing the number of attempts to remove and attach devices. Finally, the arm module contains up to six devices, and it can be confirmed that the connection can be determined by repeatedly detaching and reattaching devices, in the same way, ⑧).

B. Evaluation of Method of Generating Getting up Motions

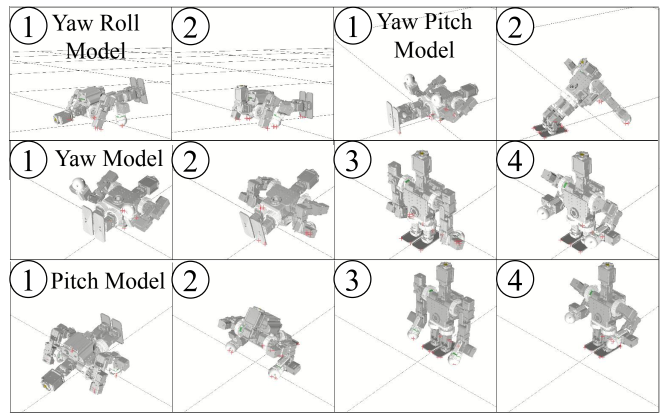

Fig. 9: Evaluation of Pseudo-Generalized Motion.

We present the pseudo-generalization of the standing-up motion and the evaluation experiment of the motion feasibility judgment in Fig.9. This experiment uses four different models of humanoids with different leg DOF configurations in a simulator that is also used in [8] and evaluates the generalization and feasibility judgment of the motion. In this section, we evaluate the feasibility of executing actions A, B, and C shown in the subsecrefsubsec:morphable-statenet for the link length and antigravity joints in four different body structures ("Yaw-Roll", "Yaw-Pitch", "Yaw", and "Pitch"). The decision is made by analytically solving for the existence of joint angles that take the desired contact state. First, motion A is to make the feet parallel to the ground, but in "Yaw-Roll," the shoulder joint is the closest antigravity joint to the feet and is also far from the feet, so it is not possible to make the feet parallel to the ground while placing the hands on the environment. Next, the "Yaw-Pitch" can complete the "Motion B," but the transition is stopped in the middle because there is no solution for the shoulder joints to be above the foot level. After all, the torso is long compared to the arms. Finally, motion C is a motion to move to the initial posture by releasing the hand tip. In both "Yaw" and "Pitch," the arm is short enough about the torso, and only the wrist joint at the end of the arm is moved, and the rest of the arm can be in contact by taking the origin posture, so both can move to the initial state. The trajectories satisfying these motions A, B, and C were calculated analytically, and the validity of the trajectories was verified using a robot model with the same mesh geometry and joint torques and velocities as the actual robot.

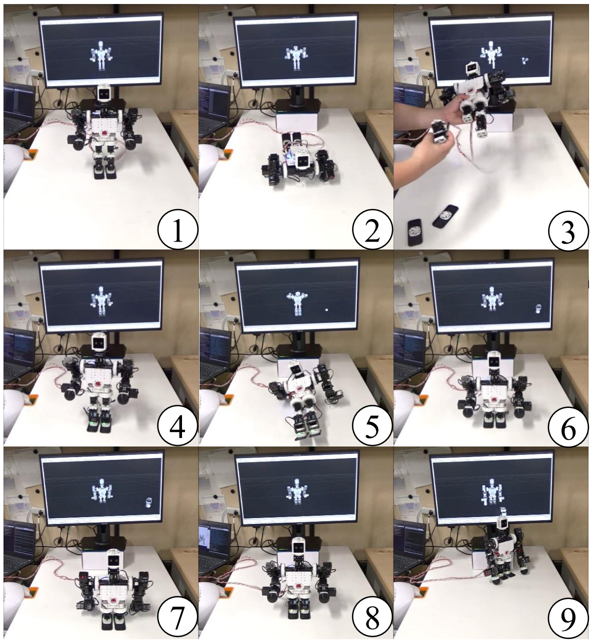

Fig. 10: Overview of Sequencial Standing Up Motions of Humanoid with Variable Structure.

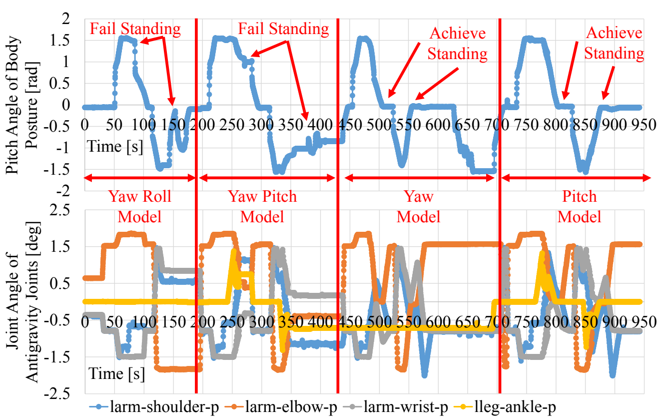

Fig. 11: Result of Whole Sequencial Standing Up Motions.

C. Evaluation of Motions with Morphable StateNet

As shown in Fig.10, the robot executes the getting-up motion in Morphable StateNet, which changes according to the body state, while interactively reconfiguring the four different robot body forms whose motions were verified. Robots with the "Yaw Model" and "Pitch Model" achieved motions those achieved in the simulator. And the robots with the "Yaw-Roll Model" and "Yaw-Pitch Model" achieved only feasible motions. In this study, the movements were coarser and longer in duration than in the simulator because purely static transitions were assumed. Throughout the entire experiment, the body was able to perform the multi-point contact motion without separation, even though it was subjected to a moment in the magnetic desorption mechanism provided by the body. On the other hand, as in the visualization experiment, the joining of new body elements often failed, and the operator repeatedly detached and connected the elements while checking the visualization screen to obtain a normal connection state.

VI. Discussion

The results of the experiments conducted in this paper are discussed. First, in the evaluation experiment of the Module Chain generation method in subsecrefexp:eval-modulechain, we were able to visualize the dynamic module detachment. On the other hand, there was a case in which device detection could not be performed properly. To solve this problem, it is possible to devise a method of arranging the electrodes so that the terminal for the communication line is always connected before the terminal for the power supply.

Next, for the verification of the deformation behavior in the simulator in Subsection V-B, it was possible to confirm that the link lengths are sufficient to achieve the desired contact state by analytically calculating the key pose of the standing-up motion using only the anti-gravity joints. On the other hand, in this method, we use only simplified version of the body link shapes. If the end-effector shape is complex, it is considered necessary to consider interference with the environment and create a space for the contact state.

Finally, the verification of the standing-up motion in the actual robot in theSubsection V-C, we were able to realize the standing-up motion according to the structure while reconfiguring the body structure. The end-effector of the robot used in this experiment was made of resin, and the coefficient of friction between the end-effector and the desk used as the environment was sufficiently small to allow the robot to transition to the supporting polygon while maintaining contact with it. On the other hand, since the friction coefficient increases depending on the end-effector shape and the material of the environment, it will be important to reduce friction by smoothing the link shape of the contact point to slide or by using the wheels equipped with the morpho-changeable humanoid as contact points to perform in a variety of environments.

VII. Conclusion

In this paper, we propose Morphable StateNet with quasi-static motion trajectories corresponding to the edge of the StateNet used for humanoid standing-up motion as StateNet with pseudo-generalized edges by making functions under certain contact conditions. This enables us to analytically calculate the feasibility of quasi-static motion trajectories described by functions for robots with various degrees of freedom and link lengths. The feasibility of the calculated motion trajectories was also demonstrated by executing the calculated getting-up trajectories while reconfiguring an actual robot. In the future, we would like to apply this method to the rise motion of a robot with more degrees of freedom in its legs and to the deformation motion of a morpho-variable robot equipped with wheels.

REFERENCES

[1] F. Kanehiro, M. Inaba, H. Inoue, and S. Hirai, “Developmental realization of whole-body humanoid behaviors based on statenet architecture containing error recovery functions,” in *Proceedings of the 2000 IEEE-RAS International Conference on Humanoid Robots (Humanoids2000)*, 2000.

[2] Y. Kakiuchi, M. Kamon, N. Shimomura, S. Yukizaki, N. Takasugi, S. Nozawa, K. Okada, and M. Inaba, “Development of life-sized humanoid robot platform with robustness for falling down, long time working and error occurrence,” in *Proceedings of the 2017 IEEE/RSJ International Conference on Intelligent Robots and Systems (IROS2017)*. IEEE, 2017, pp. 689–696.

[3] Y. Kuniyoshi, Y. Ohmura, K. Terada, A. Nagakubo, S. Eitoku, and T. Yamamoto, “Embodied basis of invariant features in execution and perception of whole-body dynamic actions-knacks and focuses of roll-and-rise motion,” *Robotics and Autonomous Systems*, vol. 48, no. 4, pp. 189–201, 2004.

[4] M. Hayashi, T. Sagisaka, Y. Ishizaka, T. Yoshikai, and M. Inaba, “Development of functional whole-body flesh with distributed three-axis force sensors to enable close interaction by humanoids,” in *Proceedings of the 2007 IEEE/RSJ International Conference on Intelligent Robots and Systems (IROS2007)*. IEEE, 2007, pp. 3610–3615.

[5] K. Kojima, Y. Kojio, T. Ishikawa, F. Sugai, Y. Kakiuchi, K. Okada, and M. Inaba, “A robot design method for weight saving aimed at dynamic motions:design of humanoid jaxon3-p and realization of jump motions,” in *Proceedings of the 2019 IEEE-RAS International Conference on Humanoid Robots (Humanoids2019)*. IEEE, 2019, pp. 617–624.

[6] F. Negrello, M. Garabini, M. G. Catalano, P. Kryczka, W. Choi, D. G. Caldwell, A. Bicchi, and N. G. Tsagarakis, “Walk-man humanoid lower body design optimization for enhanced physical performance,” in *Proceedings of the 2016 IEEE International Conference on Robotics and Automation (ICRA2016)*. IEEE, 2016, pp. 1817–1824.

[7] M. Murooka, K. Okada, and M. Inaba, “Optimization-based posture generation for whole-body contact motion by contact point search on the body surface,” *IEEE Robotics and Automation Letters*, vol. 5, no. 2, pp. 2905–2912, 2020.

[8] S. Noda, Y. Kakiuchi, H. Takeda, K. Okada, and M. Inaba, “Goal-oriented simulation-based motion interpolator for complex contact transition: Experiments on knee-contact behavior,” in *Proceedings of the 2018 IEEE-RAS International Conference on Humanoid Robots (Humanoids2018)*. IEEE, 2018, pp. 1–7.

[9] K. Nguen, Y. Kojio, S. Noda, F. Sugai, K. Kojima, Y. Kakiuchi, K. Okada, M. Inaba, *et al.*, “Dynamic fall recovery motion generation on biped robot with shell protector,” *IEEE Robotics and Automation Letters*, vol. 6, no. 4, pp. 6741–6748, 2021.

[10] S. Noda, f. Sugai, K. Kojima, K. Nguyen, Y. Kakiuchi, K. Okada, and M. Inaba, “Semi-passive walk and active walk by one bipedal robot: Mechanism, control and parameter identification,” *International Journal of Humanoid Robotics*, vol. 17, no. 02, p. 2050012, 2020.

[11] G. C. Haynes, D. Stager, A. Stentz, V. Weghe, J. Michael, B. Zajac, H. Herman, A. Kelly, E. Meyhofer, D. Anderson, *et al.*, “Developing a robust disaster response robot: CHIMP and the robotics challenge,” *Journal of Field Robotics*, vol. 34, no. 2, pp. 281–304, 2017.

[12] H. Bae, I. Lee, T. Jung, and J. Oh, “Walking-wheeling dual mode strategy for humanoid robot, DRC-HUBO+,” in *Proceedings of the 2016 IEEE/RSJ International Conference on Intelligent Robots and Systems (IROS2016)*, 2016, pp. 1342–1348.

[13] T. Makabe, K. Okada, and M. Inaba, “Development of the Assembling System for Structure Transformable Humanoid with Attach-Lock-Detachable Magnetic Coupling (in press),” in *Proceedings of the 2024 IEEE-RAS International Conference on Robotics and Automation (ICRA2024)*.

[14] “KRS Servomotor Series (KONDO KAGAKU CO. LTD).” https://kondo-robot.com/product-category/servomotor/krs.

[15] T. Makabe, N. Hiraoka, S. Noda, T. Anzai, K. Kimura, M. Hattori, H. Sato, F. Sugai, Y. Kakiuchi, K. Okada, and M. Inaba, “Design and Development for Humanoid-Vehicle Transformer Platform with Plastic Resin Structure and Distributed Redundant Sensors,” in *Proceedings of the 2022 IEEE-RAS International Conference on Robotics and Automation (ICRA2022)*. IEEE, 2022, pp. 8526–8532.

[16] “IR Proximity Sensor: VCNL4040,” https://www.vishay.com/docs/84274/vcnl4040.pdf.

[17] “ROS wiki:tf,” https://wiki.ros.org/tf.